NASA CR-165167

(NASA-CR-165167) GaAs SHALLOW-HOMOJUNCTION SOLAR CELLS Final Report (Lincoln Lab.) 29 p HC A03/MF A01 CSCL 10A N81-15463

Unclas G3/44 29668

Final Report

J. C. C. Fan

GaAs Shallow-Homojunction Solar Cells

30 June 1980

Prepared for National Aeronautics and Space Administration under Contract NAS C-30068-0 by

Lincoln Laboratory

MASSACHUSETTS INSTITUTE OF TECHNOLOGY

LEXINGTON, MASSACHUSETTS

ABSTRACT

With the objective of demonstrating the feasibility of fabricating 2- × 2-cm efficient, shallow-homojunction GaAs solar cells for space applications, this program has been addressing the basic problems of material preparation and device fabrication. Significant progress has been made and conversion efficiencies close to 16 percent at AM0 have been obtained on 2- × 2-cm cells. Measurements and computer analyses on our $n^+/p/p^+$ shallow-homojunction cells indicate that such cell configuration should be very resistant to 1-MeV electron irradiation.

PRECEDING PAGE BLANK NOT FILMED

CONTENTS

ACKNOWLEDGMENTS

This work was performed with the collaboration of C.O. Bozler, R.L. Chapman, F.M. Davis, R.P. Gale, R.W. McClelland, B.J. Palm, and G.W. Turner. The tecnnical assistance of M.K. Connors, G.H. Foley, and O. Hurtado is sincerely appreciated.

GaAs SHALLOW-HOMOJUNCTION SOLAR CELLS

The objective of this program is to develop CVD growth processes and device fabrication techniques so as to produce 2- × 2-cm GaAs space-resistant homojunction solar cells with efficiencies above 14 percent at AM0. This report summarizes the results achieved during the one-year program starting in July 1979.

I. INTRODUCTION

Although Si solar cells have been extensively used in space, GaAs cells are now emerging as promising candidates for space applications with a number of potential advantages over Si cells. Since the absorption length for sunlight in GaAs is only about 2 μm (see Ref. 1), two orders of magnitude less than in Si, GaAs cells should exhibit less radiation damage in space, because damage generated more than a few absorption lengths beneath the surface should have little effect on photocurrent collection. In addition, the theoretical conversion efficiency is higher for GaAs than for Si (see Ref. 2), and GaAs cells operate better than Si cells at elevated temperatures[2] and high solar concentrations.[3] Furthermore, the stronger absorption of sunlight in GaAs should allow a significant reduction in cell thickness and, therefore, weight. We have previously reported[4] the results of experiments on the resistance of shallow-homojunction GaAs cells (size 1 × 0.5 cm) to 1-MeV electron irradiation. These results are highly encouraging, suggesting that such cells could be more resistant to the radiation of the space environment than either Si cells or GaAlAs/GaAs heteroface cells, the GaAs solar cells that until now have been of most interest for space applications.

The GaAlAs/GaAs heteroface cells[5-7] incorporate a Zn-doped[6] or Be-doped[7] p-GaAlAs window layer grown by liquid-phase epitaxy on an n-GaAs wafer. During growth of the window layer, the p dopant diffuses into the n substrate producing a p-n homojunction generally more than 0.5 μm deep. The layer of GaAlAs greatly reduces the recombination velocity at the GaAs surface while transmitting most of the solar spectrum. Single-crystal cells have been fabricated with efficiencies as high as 22 percent at AM1 (see Ref. 8). However, irradiation with high-energy electrons, the most important source of radiation damage to solar cells in the space environment, causes a strong decrease in the photocurrent, partly because the diffusion lengths of minority carriers in the p and n layers are decreased and partly because the surface recombination velocity at the GaAlAs/GaAs interface is increased.[6] These detrimental effects can be greatly reduced by fabricating GaAs solar cells that utilize a shallow-homojunction $n^+/p/p^+$ structure without a GaAlAs layer.

We have developed such shallow-homojunction solar cells, with conversion efficiencies of 20 to 21 percent at AM1, that incorporate GaAs layers grown by chemical vapor deposition (CVD) on either GaAs (Ref. 9) or Ge (Ref. 10) single-crystal substrates. The cell structures are shown in Fig. 1. In these devices, surface recombination losses are reduced because the n^+ layer – doped with S – is so thin (~1000 Å) that most of the photogenerated carriers are created in the p layer – doped with Zn – below the junction. Because the n^+ layer is so thin, almost all the electron damage effects will occur in the p layer, where the minority-carrier diffusion length is much longer (~20 μm) than the solar absorption length (~2 μm). We have confirmed this superior radiation resistance in a series of experiments using 1-MeV electrons.[4]

The goal of this program is to develop techniques of fabricating GaAs space cells of the standard size of 2 × 2 cm for a series of experiments to be performed at NASA. Cells of the

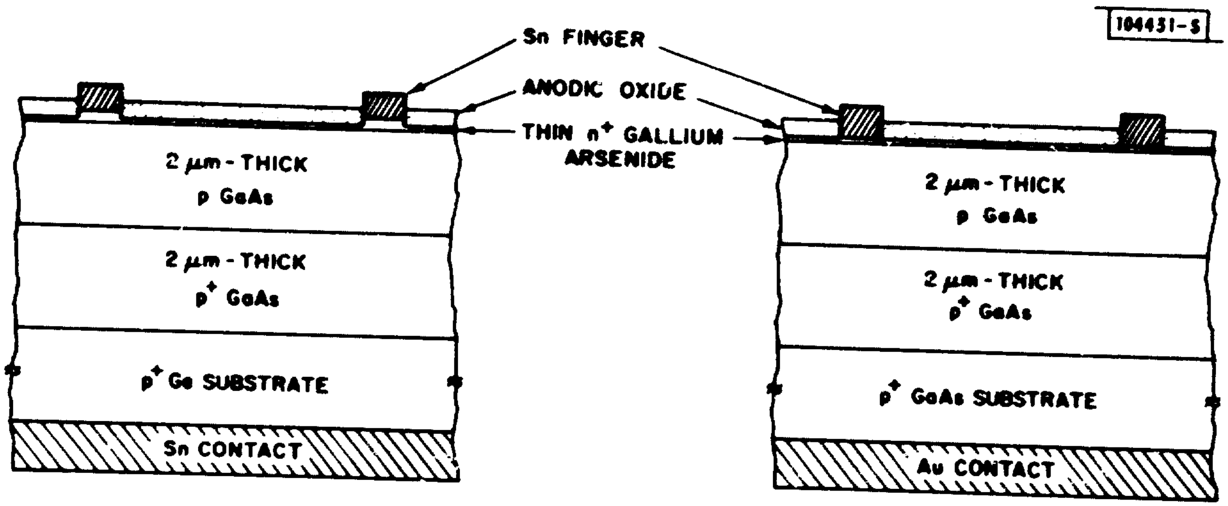

Fig. 1. Schematic diagram of GaAs shallow-homojunction solar cells on GaAs or Ge substrates.

required size and required conversion efficiencies were successfully produced, and preliminary experiments on these cells at NASA confirmed our earlier results on the much smaller cells. This report will concentrate on the material growth and device fabrication of such 2- × 2-cm cells, as well as some computer calculations of the optimal design for a highly space-resistant GaAs shallow-homojunction solar cell.

II. MATERIAL GROWTH

A. Experimental Procedures

We have constructed a CVD system solely dedicated to the growth of GaAs homojunctions. This system (shown in Fig. 2), which employs the $AsCl_3$ method with a fused-silica reactor, is similar to the one that is used at Lincoln Laboratory for the epitaxial growth of GaAs structures for microwave devices. The reactor tube has an inner diameter of 55 mm, and the H_2 flow through the $AsCl_3$ evaporator and over the Ga boat is in the range 300 to 500 cm^3/min. Some of our cells were deposited using this $AsCl_3$-Ga-H_2 liquid source method, while lately we have been using the $AsCl_3$-GaAs-H_2 solid source method. The advantages of using solid source will be described later. The p and n dopants are introduced in the vapor phase by using $(CH_3)_2Zn$ and H_2S, respectively. The reactor tube is vertical, and the substrates are supported on a quartz pedestal which rotates, thus resulting in greater doping uniformity in the layers. The pedestal is large enough for substrates with a diameter of 4.4 cm. Under high purge flows, the reactor tube can be opened at the bottom to load and unload substrates without losing the H_2 atmosphere inside the tube. Thus, the furnace can remain at growth temperature during the loading procedure, decreasing the cycle time between runs. Once inside the reactor tube, the substrate can be preheated in pure H_2 just before being introduced into the reactant gas flow at the growth position.

Just prior to loading, polished GaAs substrates oriented 2° off (100) toward (011) were cleaned in acetone, trichloroethylene, acetone, deionized (DI) water, sulfuric acid, and DI water. The substrate was then etched for one minute in 5:1:1 H_2SO_4, H_2O_2, H_2O at 20°C and rinsed in DI water, at which point the uniform coverage by the water was used as one indication that the substrate was clean. It was dried with nitrogen and loaded into the reactor.

Two types of layers were grown and characterized for this work: p layers (about 2 to 3 μm thick) on semi-insulating substrates, and $n^+/p/p^+$ structures on p^+ substrates. The $n^+/p/p^+$ structures typically have thicknesses as follows: $n^+ \sim 0.2$ μm, $p \sim 2$ to 3 μm, and $p^+ \sim 2$ μm. The p-type layers were cleaved to provide pieces for diffusion and lifetime measurements performed at NASA. The $n^+/p/p^+$ solar cell structures were mostly grown on rectangular wafers 2.5 cm wide by 4.5 cm long, doped with Zn to 2×10^{18} cm^{-3}. After growth, a piece 2.5 × 2.5 cm was cleaved from each wafer for the 2- × 2-cm cell fabrication. The remaining pieces were used for other characterization purposes.

B. Growth Over Large Areas

Since the conversion efficiency of a shallow-homojunction cell is sensitive to the thickness of the n^+ layer, the n^+ layer must be uniformly thick over the cell area. This was found to be the case when we measured uniform current response over the area of the finished cells.

Two surface-related problems were encountered in growing the large-area cells. The first problem was closely related to surface cleaning and polishing over this large area. Poor surface preparation results in surface haze and the growth of hillocks. The surface haze does not

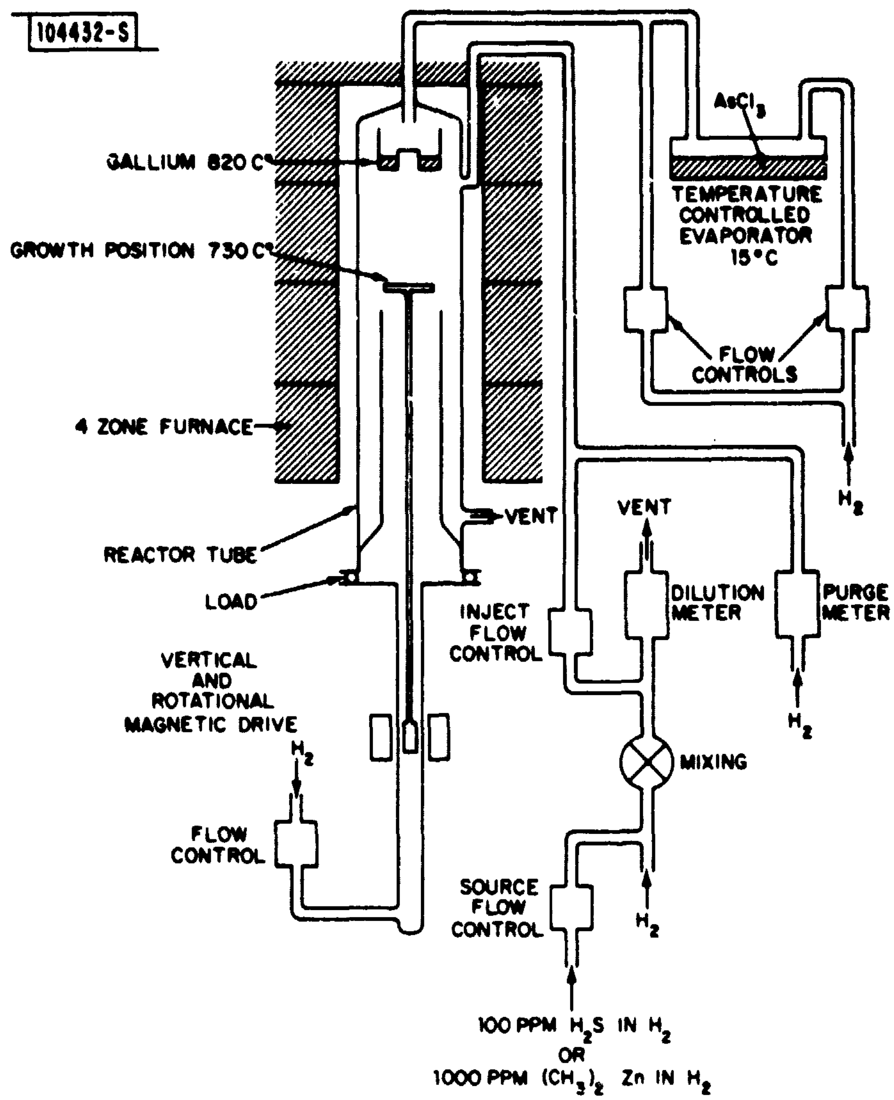

Fig. 2. Schematic diagram of GaAs vapor deposition system showing H_2, $AsCl_3$, and doping gases flow control, and also a cross-sectional view of reactor tube.

appear to cause major problems to cell efficiency, but hillocks are quite detrimental. The second problem was the appearance of slip lines on these large wafers after growth. The cause of slip lines was traced to thermal stress which is apparently more prevalent in large-area wafers, and can be eliminated by proper heating and cooling of the wafers.

C. Layer Characteristics

Seven 2- × 2-cm $n^+/p/p^+$ cells were delivered to NASA. Table I lists the doping levels and thicknesses of the p and p^+ layers. These two material parameters were intentionally changed so as to examine the radiation resistance of such cells. The n^+ layer was doped to 4 to 5 × 10^{18} cm^{-3} and was about 0.2 μm thick. The n^+ layer characteristics were kept the same for all the cells. The finished cells, however, had thinner n^+ layers (~500 to 700 Å) for high cell efficiencies. The subsequent thinning procedure will be discussed in a later section on cell fabrication.

TABLE I

DOPING LEVELS AND THICKNESSES OF p AND p^+ LAYERS ON $n^+/p/p^+$ CELLS

Cell Number	p Layer		p^+ Layer	
	Doping (cm^{-3})	Thickness (μm)	Doping (cm^{-3})	Thickness (μm)
5426	3.7E16	1.8	3.5E18	1.7
5348	5.6E17	2.3	5.0E18	2.2
5344	5.6E17	3.0	5.0E18	2.8
5340	4.0E17	2.6	4.0E18	2.0
5245	1.5E17	2.6	4.0E18	2.1
5240	1.5E17	3.1	5.0E18	2.4
5239	1.5E17	3.2	5.0E18	2.7

D. Use of Solid GaAs Source Material

Traditionally, the $AsCl_3$ method uses a liquid Ga source. We have carried out a series of experiments that used a solid GaAs source which was cut from an undoped polycrystalline ingot (from Crystal Specialties, Inc.) with intergrain Hall mobilities greater than 5000 cm^2/V-s at room temperature. Background carrier concentrations of epitaxial layers were found to be n-type and were in the mid-10^{15} cm^{-3} range. The Hall mobilities of these layers were greater than 5500 cm^2/V-s at room temperature. One of the seven cells delivered, number 5426, was grown with the solid source and exhibited the same excellent characteristics as the other six cells that were grown with a Ga liquid source.

There are many advantages of the solid source over the liquid source. For example, arsenic saturation, necessary when the Ga source is used, is eliminated. Therefore, not only the growth time is shortened, but one ampoule of $AsCl_3$, with the solid source, can produce many more films. In addition, background doping is found to remain almost constant throughout the duration of solid source charge, while the liquid source is more capable of dissolution of

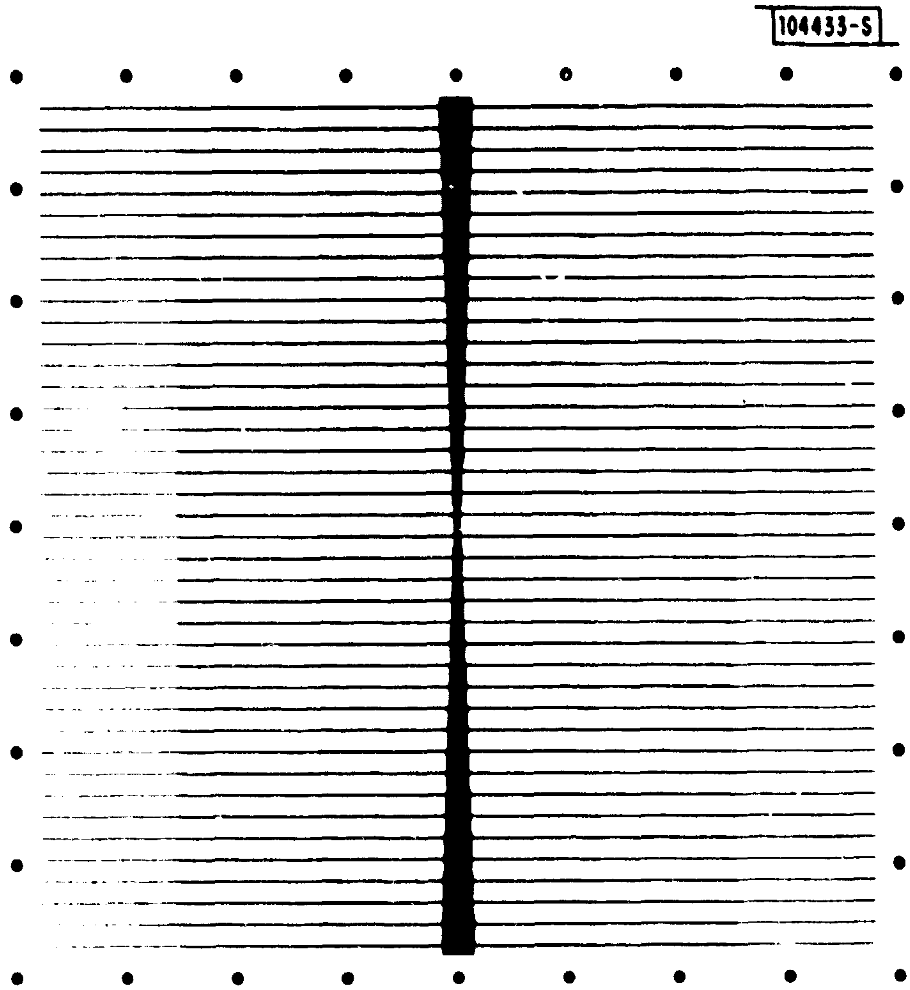

Fig. 3. Schematic diagram of front contact mask. Small circular dots at perimeter of mask are contact dots for small test mesa cells.

impurities resulting in an increase in background doping over time. Finally, by using the solid source, the chemical reactions are more efficient and have fewer reaction by-products. The reactor was also found to stay clean for a much longer time. The interval between reactor cleanings is now about a factor-of-four times longer.

III. DEVICE FABRICATION

A. Fabrication of GaAs Shallow-Homojunction Solar Cells

The fabrication technology of high-efficiency GaAs shallow-homojunction solar cells having areas up to 0.5 × 1.0 cm is well developed. Previous publications[9,10] described fabrication details leading to GaAs solar cells having conversion efficiencies of up to 20 to 21 percent (AM1). Unique advantages in the fabrication of these cells include the lack of any vacuum processing steps as well as the growth of an anodic oxide directly on the GaAs surface. The anodization reduces the n^+ epitaxial layer thickness (to optimize the photocurrent) and forms an anodic oxide layer which serves as an effective antireflection coating for the completed solar cell.

The fabrication of 2- × 2-cm GaAs shallow-homojunction solar cells was based on these same techniques. Some changes were made in the details of certain process steps, and these will be described.

B. Fabrication of 2- × 2-cm GaAs Shallow-Homojunction Solar Cells

The fabrication of the 2- × 2-cm solar cells first required the generation of suitable masks to be used in the photolithography. A front contact grid mask and an active area definition mask were required, as well as a special mask to cover the front contact metallization during anodization. The front contact mask (Fig. 3) was designed with a large control bus bar of the "bow tie" geometry, with 40 tapered fingers spaced along the bus bar to minimize series resistance losses. The various geometries of this mask were designed for use with electroplated Sn (between 3 to 4 μm thick).

The first step in fabricating a 2- × 2-cm cell was the electroplating of the back Au contact. The front of the sample was then covered with positive photoresist, and the front contact pattern was opened using the front contact mask. The front Sn contact was then electroplated. The active area of the cell was defined with the mesa mask, and areas surrounding this mask were etched below the junction.

The final fabrication step was the anodization. The GaAs was anodized in a solution of water, glycol, and tartaric acid.[9] The anodization was performed at room temperature under constant current conditions. Using a current density of 1 mA/cm^2, 13 Å/V of GaAs was converted to 20 Å/V of anodic oxide. A final anodization of 43 V gave the best antireflection coating.

A difficulty in uniformly anodizing the GaAs surface with the Sn contact grid present was discovered with the 2- × 2-cm cells. Since the Sn is also oxidizing in a competing reaction, it was found that the anodic oxide grown on GaAs near areas of high Sn coverage tended to be thinner than oxides grown on areas away from the Sn.

Two solutions to this problem were tried. In the first, the initial current density was increased by an order of magnitude, and the anodization proceeded rapidly. By monitoring the rate of voltage rise on an x-y recorder, the current density could be controlled to yield a more uniform anodic oxide. However, due to the inability to control this process exactly, a second approach was developed in which the Sn metallization was covered with photoresist using a special

mask which left the GaAs surface uncovered. Anodization of this type of protected cell was very reproducible, although it did require an additional process step.

By measuring the AM1 photocurrent after the initial anodization, the n^+ layer thickness and the optimum anodization sequence were determined. The anodic oxide was removed between anodization steps with a mild HCl solution which did not etch the GaAs.

Although excellent 2- × 2-cm cells have been fabricated, we are currently investigating appropriate techniques which would allow us to anodize the n^+ surface, in the presence of Sn contacts, without having to use the protective photoresist. In addition, alternative antireflection coatings such as Si_3N_4, that are even better optically matched for GaAs solar cells, are being developed.

IV. CELL CHARACTERIZATION

Cell efficiency measurements, using an Oriel AM0 solar simulator, were made on seven 2- × 2-cm cells fabricated from wafers that have different cell configurations, as described in Table I. The incident intensity was adjusted to 135.3 mW/cm^2, using a NASA-measured GaAs solar cell as a reference. The cells were mounted on a copper block which was thermoelectrically controlled to 25°C. Table II lists the characteristics of the cells.

TABLE II

SOLAR CELL EFFICIENCY MEASUREMENTS (AM0)

Cell Number	J_{sc}	V_{oc}	ff	η
5426	26.1	0.983	0.78	14.7
5348	25.1	0.985	0.82	14.9
5344	26.4	0.983	0.81	15.6
5340	24.4	0.966	0.78	13.6
5245	25.8	0.983	0.81	15.1
5240	27.1	0.968	0.76	14.7
5239	27.0	0.958	0.78	15.0

J_{sc} = short-circuit current density (mA/cm^2)

V_{oc} = open-circuit voltage (V)

ff = fill factor

η = cell efficiency (percent) (includes contact bars and fingers)

The external quantum efficiency, which is the ratio of the number of carriers collected (I_{sc}/q) to the number of incident photons, was measured. The value of short-circuit current I_{sc} and incident photon flux were measured as a function of wavelength in a spectrometer which

was arranged so that all the light fell between two contact fingers. Figure 4 illustrates the quantum efficiency of one of the seven cells. The other six cells have similar characteristics. We have integrated the quantum efficiency curves of five of the cells with the published AM0 spectrum,[11] and found the calculated short-circuit current density J_{sc} of the cells (after the contact shadowing was considered) to be close to those measured using the AM0 solar simulator (as shown in Table III). The close agreement not only indicates that our cell efficiency and quantum efficiency measurements are internally consistent, but also confirms that the cell response of our cells is uniform to a few percent across the 2- × 2-cm area. This latter property was confirmed by mapping photocurrent response of one of the cells with a scanning He-Ne laser beam. Figure 5 shows the response of such a cell; the irregular trace in the middle was caused by the center bus bar.

TABLE III

MEASURED J_{sc} UNDER AM0 SIMULATION, AND CALCULATED J_{sc} OBTAINED FROM INTEGRATING QUANTUM EFFICIENCY

Cell Number	Measured J_{sc} (mA/cm^2)	Calculated J_{sc} (mA/cm^2)
5426	26.1	23.8
5348	25.1	26.2
5344	26.4	27.7
5340	24.4	25.2
5245	25.8	26.8

V. ELECTRON IRRADIATION RESULTS

The electron irradiation results on the seven 2- × 2-cm cells have just been completed at NASA, and the results are similar to those that were performed on 0.5- × 1-cm cells. Although the results on the smaller-area cells have already been published,[4] we will briefly describe those results and some recent computer analyses of those results.

Four $n^+/p/p^+$ GaAs cells, each about 0.5 cm^2 in area, were tested under 1-MeV electron irradiation. They were fabricated with Au or Sn front contacts and with an Au back contact. Table IV lists structural characteristics of the four cells. Electron irradiation at normal incidence was provided by a Dynamitron electron accelerator. Samples were irradiated individually by mounting them next to the aperture of a Faraday cup so that all fluences were measured directly. The cells were open-circuited and at room temperature during irradiation. The electron flux density was kept at about 10^{12} e/cm^2s, low enough to avoid significant cell heating. Cell conversion efficiencies before and after irradiation were measured at about 25°C with the AM0 solar simulator. Quantum efficiency measurements were made at wavelengths from 0.40 to 0.90 μm. No thermal annealing was employed between successive electron irradiations, and no self-annealing effects were observed during the time intervals between irradiations.

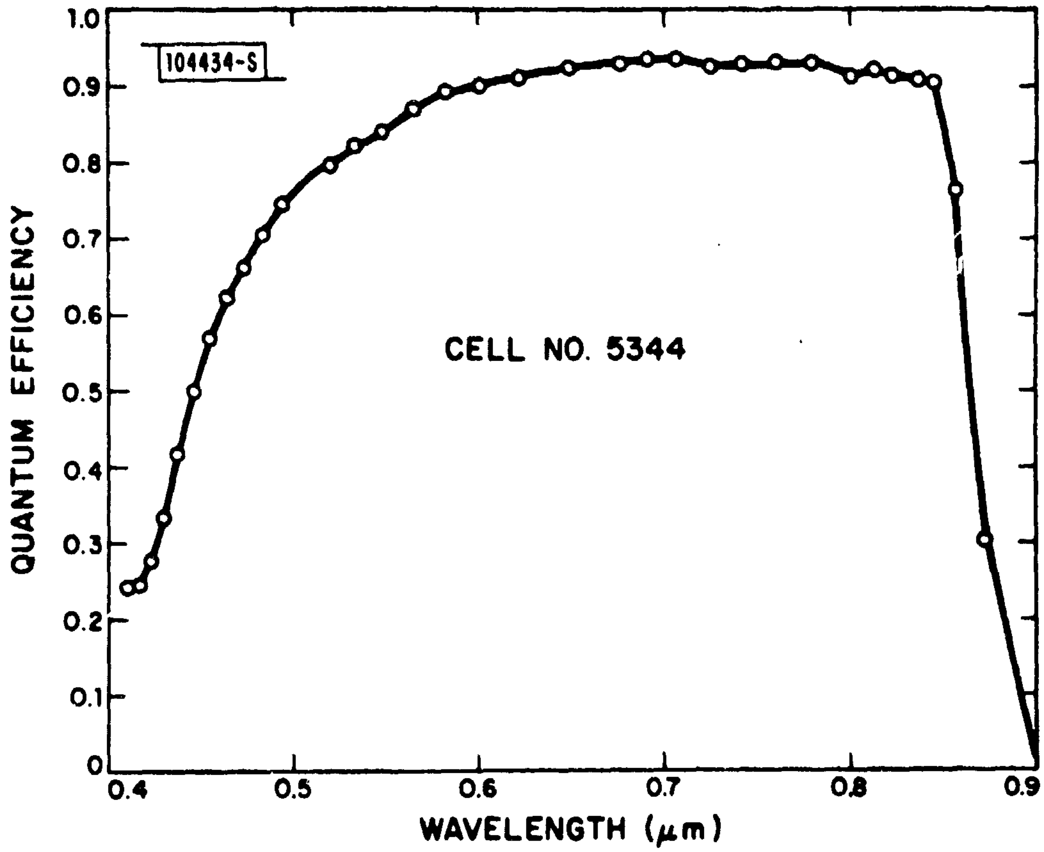

Fig. 4. Quantum efficiency of one of seven cells delivered to NASA.

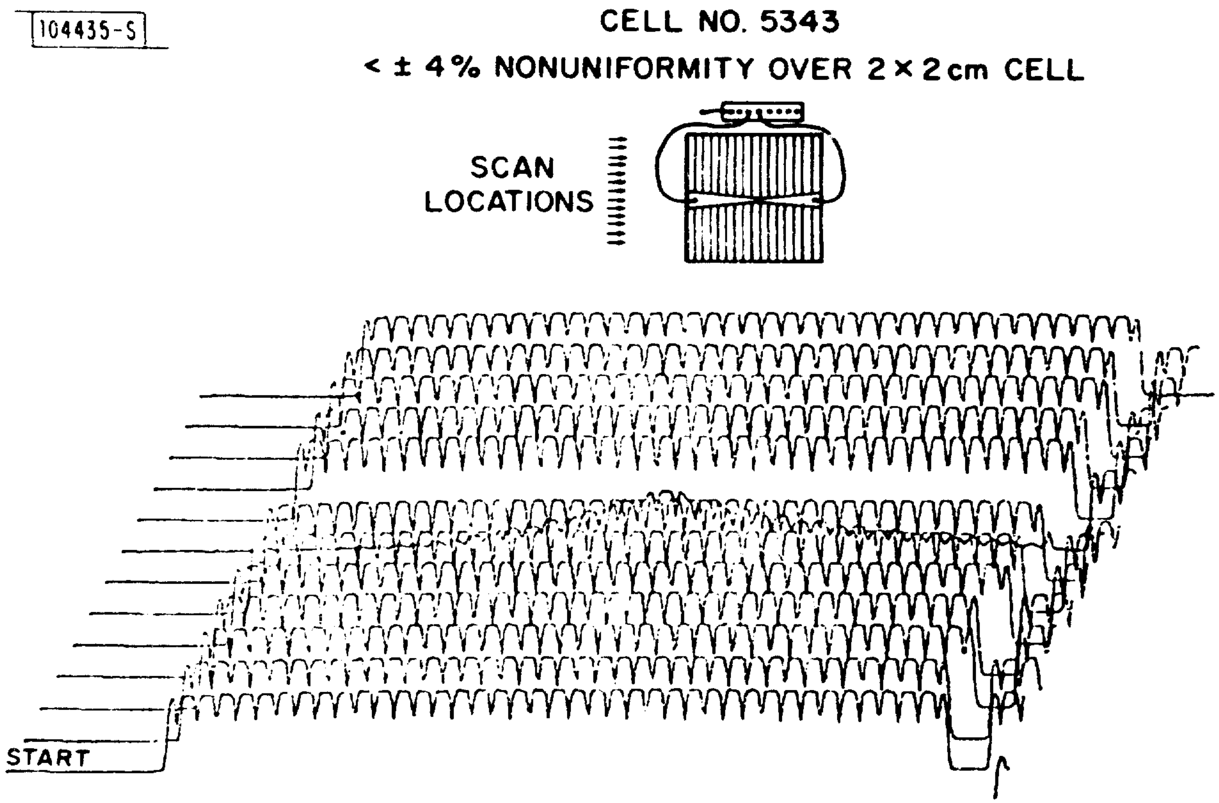

Fig. 5. Photocurrent response of a 2- × 2-cm cell, measured with a scanning He-Ne laser.

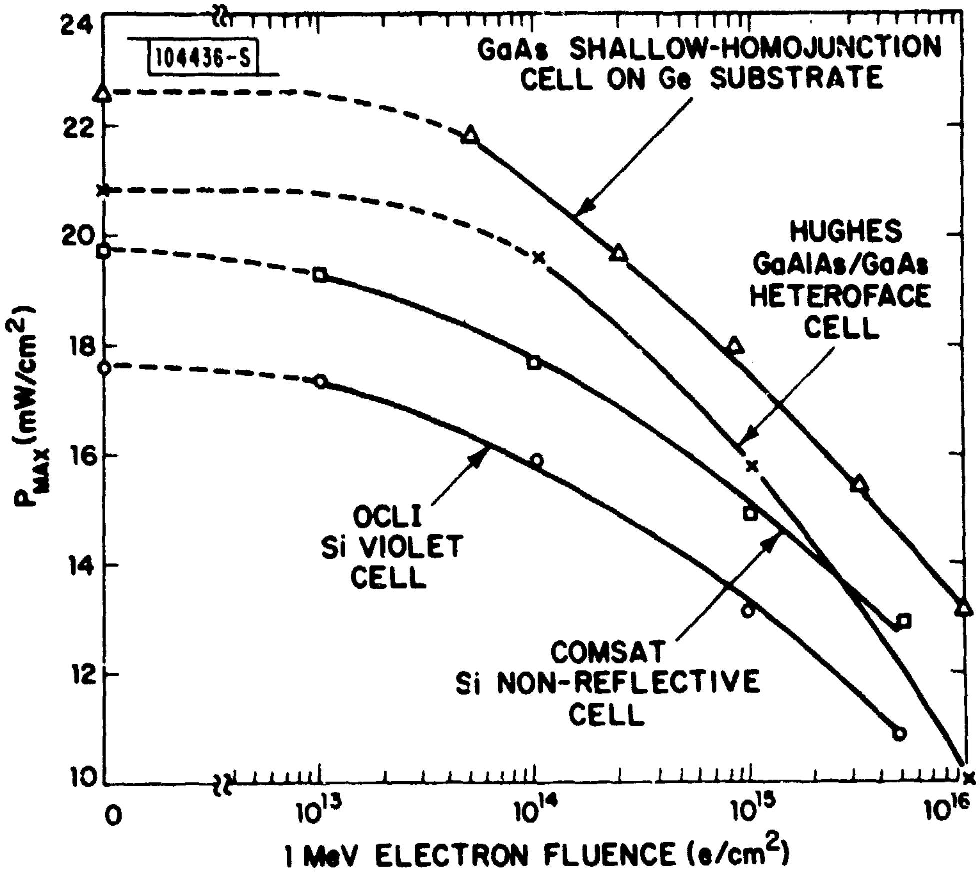

Fig. 6. Maximum output power density at AM0, P_{max}, for cell 1 as a function of cumulative electron fluence. Results for three other types of cells made by OCLI (Ref. 12), COMSAT (Ref. 12), and Hughes (Ref. 13) are included for comparison.

TABLE IV STRUCTURAL CHARACTERISTICS OF FOUR SHALLOW-HOMOJUNCTION GaAs SOLAR CELLS TESTED UNDER 1-MeV ELECTRON IRRADIATION								
Cell Number	n^+ Layer		p Layer		p^+ Layer		Substrate	Front Contact
	n (cm^{-3})	t (μm)	p (cm^{-3})	t (μm)	p (cm^{-3})	t (μm)		
1	5×10^{18}	~0.05	1×10^{17}	2.0	5×10^{18}	2.0	Ge	Au
2	5×10^{18}	~0.1	1×10^{15}	1.0	5×10^{16}	1.0	GaAs	Au
			1×10^{16}	1.0				
3	5×10^{18}	~0.1	1×10^{17}	2.0	5×10^{18}	2.0	GaAs	Au
4	4×10^{18}	~0.05	3×10^{17}	2.5	2×10^{18}	0.5	GaAs	Sn

Figure 6 shows the maximum output power density at AM0, P_{max}, for cell 1 as a function of cumulative electron fluence. The value of P_{max} was initially over 22 mW/cm^2 (cell conversion efficiency η at AM0 of 16.7 percent), and slowly decreased to about 13 mW/cm^2 at a fluence of 10^{16} e/cm^2. Both initial and final P_{max} values are higher than those reported[12,13] for three other types of space cells, as plotted in Fig. 6. The results for the other three types, a GaAs heteroface cell and two Si cells, were obtained under similar experimental conditions, except that their areas were 4 cm^2 and the Si cells were thermally annealed at 50°C for over 24 h between successive electron irradiations.[12]

Table V lists device characteristics of cell 1 before electron irradiation and after 10^{16} e/cm^2 irradiation. Although the cell exhibits excellent radiation resistance compared with other types of cells, the values of I_{sc} and open-circuit voltage V_{oc} both decreased about 20 percent after the high electron fluence. The decrease in V_{oc} corresponds to an increase in leakage current, as indicated by an increase in saturation current density J_o from 6×10^{-18} to 1×10^{-14} A/cm^2 after

TABLE V DEVICE CHARACTERISTICS OF FOUR SHALLOW-HOMOJUNCTION GaAs SOLAR CELLS BEFORE AND AFTER 10^{16} e/cm^2 1-MeV ELECTRON IRRADIATION								
Cell Number	Initial Values				Final Values (After 10^{16} e/cm^2)			
	J_{sc} (mA/cm^2)	V_{oc} (V)	ff	η (percent)	J_{sc} (mA/cm^2)	V_{oc} (V)	ff	η (percent)
1	27.5	1.00	0.82	16.7	21.0	0.82	0.77	9.8
2	19.2	0.95	0.81	10.9	18.0	0.72	0.69	6.6
3	22.0	0.99	0.80	12.9	17.2	0.82	0.76	7.9
4	25.6	0.98	0.83	15.4	17.9	0.81	0.78	8.4

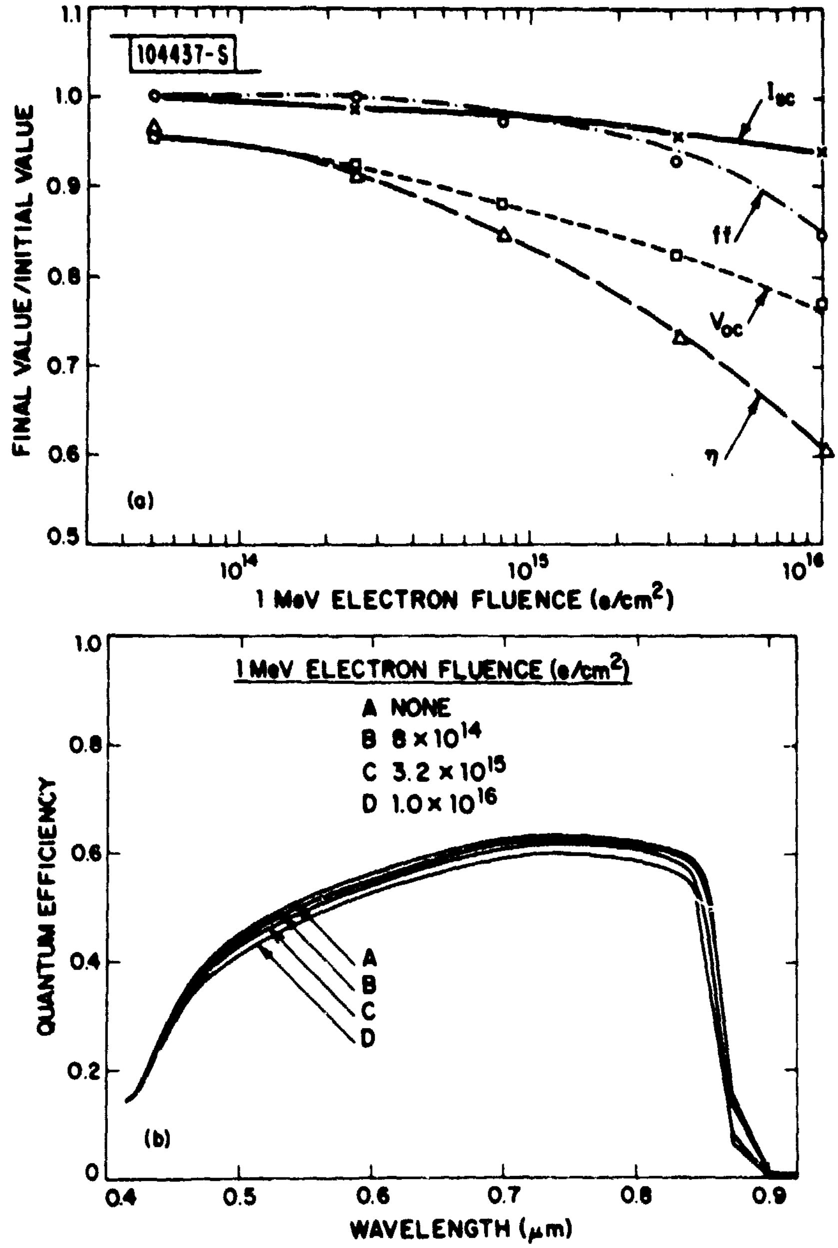

Fig. 7. (a) Characteristics of cell 2 as a function of cumulative electron fluence. (b) Quantum efficiency measurements on cell 2 at various electron fluences.

10^{16} e/cm^2 irradiation. The diode factor remained the same, however, at 1.1. The decrease in I_{sc} may be attributed partly to degradation of the electron diffusion length in the p layer of the cell. We therefore expected the I_{sc} decrease to be reduced by lowering the doping level in the p layer below the value of 1×10^{17} cm^{-3} in cell 1, in order to increase the initial electron diffusion length.

Our expectation was confirmed by the results for cell 2 which has a p doping level of 10^{15} to 10^{16} cm^{-3} and no anodic coating. Figure 7(a) shows the device characteristics of this cell after successive electron irradiations, while the initial and final values are listed in Table V. For a fluence of 10^{16} e/cm^2, I_{sc} decreased by only about 6 percent of its original value. This decrease in I_{sc} is much smaller than decreases reported for Si cells[12] or for GaAs heteroface cells.[13,14] This small decrease is confirmed by the quantum efficiency measurements on the cell at various electron fluences, as plotted in Fig. 7(b). The cell, however, still exhibits a significant decrease in V_{oc}. The diode factor changes slightly, from 1.1 before irradiation to 1.3 after 10^{16} e/cm^2 fluence, but J_o increased greatly from 2×10^{-18} to 1×10^{-11} A/cm^2.

Table V also lists the device characteristics of cells 3 and 4 before and after 10^{16} e/cm^2 electron irradiation. The results for these cells are quite similar to those for cell 1, except that they have lower initial η values.

Our experimental results for four $n^+/p/p^+$ shallow-homojunction GaAs solar cells indicate that such cells are resistant to electron irradiation. One of these cells is superior to other types of space cells, in having a higher output power density before and after 1×10^{16} e/cm^2 1-MeV electron irradiation. In a second cell, a very small change in I_{sc} was achieved by using a low doping level in the p layer and no anodic AR coating. In addition, our initial experiments indicate that shallow-homojunction GaAs cells fabricated on Ge substrates are similar to cells on GaAs substrates in their resistance to electron irradiation. The substitution of Ge for GaAs substrates will permit a major decrease in Ga consumption as well as a reduction in cell cost. Furthermore, since Ge is much stronger mechanically than GaAs, this substitution will also enable the use of thinner substrates, thus reducing the weight of the cells.

We have written a model to predict the external quantum efficiency and conversion efficiency of GaAs solar cells. The detailed features of the model were described earlier,[15] and will not be described here. However, this model was modified to study the cell performance under electron irradiation. When the 1-MeV electrons impinge on the cells, the major degradation on the cells is the creation of defects in the GaAs layers that greatly reduces the diffusion lengths and lifetimes of minority carriers. This reduction, in turn causes the V_{oc}, J_{sc}, and fill factor (ff) to decrease.

In our shallow $n^+/p/p^+$ homojunction cells, we have found that the thin n^+ layer contributes very little to the photocurrent of the cells. Therefore, the important degradation is in the p layer. It has been proposed[16] that degradation with electron fluence may be formulated in terms of:

In n layer

$$\frac{1}{L_p^2} = \frac{1}{L_{po}^2} + K_p\phi$$

$$S_p = S_{po}\left(\frac{L_{po}}{L_p}\right)^2$$

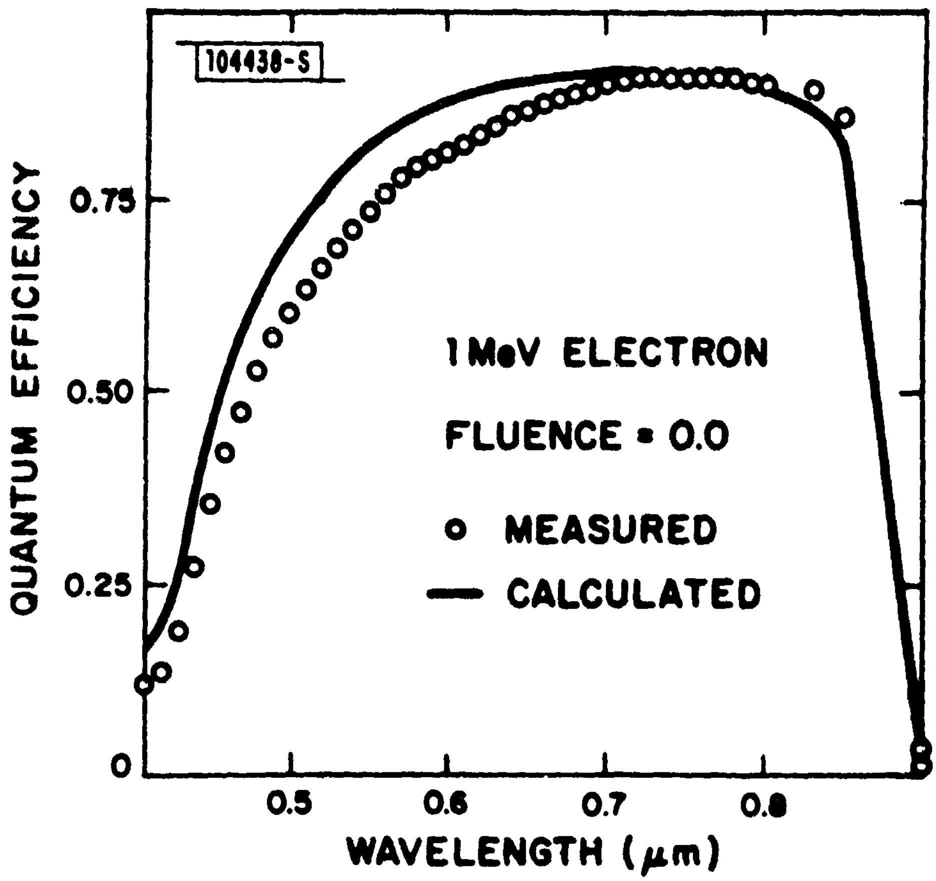

Fig. 8. Calculated and measured quantum efficiency results for cell 1 at zero electron fluence.

In p layer

$$\frac{1}{L_n^2} = \frac{1}{L_{no}^2} + K_n\phi$$

$$S_n = S_{no}\left(\frac{L_{no}}{L_n}\right)^2$$

where L_p, L_n are the minority-carrier diffusion lengths for holes and electrons after electron irradiation, L_{po}, L_{no} are the minority-carrier diffusion lengths for holes and electrons before they are irradiated, S_p and S_n are the surface recombination velocities for holes and electrons, respectively, and ϕ is the 1-MeV electron fluence (e/cm^2).

In each cell, if K_n and K_p are known, then the cell performance can be calculated for all fluences. In order to find K_n and K_p, we have treated K_n and K_p as independent adjustable parameters, and using a single value for each of these quantities, we performed computer calculations to achieve best simultaneous fit to three sets of experimental values for QE obtained in measurements at three sets of electron fluences. Figures 8, 9, and 10 show the calculated and measured QE curves for cell 1. The values for K_n and K_p used were 2.1×10^{-8}. It was found that the QE was not sensitive to the K_p values, as expected, since the n^+ layer was so thin that the cell performance was not dependent on this layer. Therefore, accurate values for K_p are difficult to obtain and, for our purposes, not necessary. Therefore, for all our calculations we have kept $K_p = 2.1 \times 10^{-8}$. The value of K_n, however, was found to depend on the doping level N_A in the p level, and using the similar fitting procedures discussed for cell 1, we have obtained the K_n values for cells 2 and 3 (see Fig. 11). The resulting K_n was found to follow approximately a linear relationship with N_A (note that cell 2 is composed of two p layers: 1 μm thick, 1×10^{15} cm^{-3}; and 1 μm thick, 1×10^{16} cm^{-3}. We used an average 5×10^{15} cm^{-3} as the value of N_A for this cell). The following relationship is obtained:

$$\log K_n = (0.77) \log N_A - 20.8 \quad .$$

Once we have obtained the K_n relationship with N_A, we could calculate the cell efficiency vs electron fluence for different N_A doping levels. Table VI shows the calculated cell characteristics before and after 10^{16} e/cm^2 for one such cell configuration as a function of N_A. (The basic cell configuration n^+ layer: 0.05-μm-thick, 5×10^{18} cm^{-3} doping level; p layer: 2 μm thick; p^+ layer: 2-μm-thick, 5×10^{18} cm^{-3} doping level; and 850-Å-thick anodic antireflection coating.) Although the AM0 efficiency has a shallow maximum at around $N_A \sim 5 \times 10^{16}$ cm^{-3}, the relative degradation in efficiency is much less for low p layers. We have not calculated for N_A less than 1×10^{15} cm^{-3} because it is presently impractical to grow layers of such p doping levels. The relative degradation effect can be best illustrated by Fig. 12, which shows a plot of the ratios of calculated AM0 efficiencies before and after 10^{16} e/cm^2 fluence as a function of N_A. For $N_A \sim 10^{15}$ cm^{-3}, the degradation is only about 20 percent. Figure 13 shows the AM0 efficiency values for these different N_A values as a function of fluences. Although cells with higher N_A values started with higher efficiency values, after about 10^{14} e/cm^2 1-MeV electron fluence, cells with lower p doping level actually have higher conversion efficiencies.

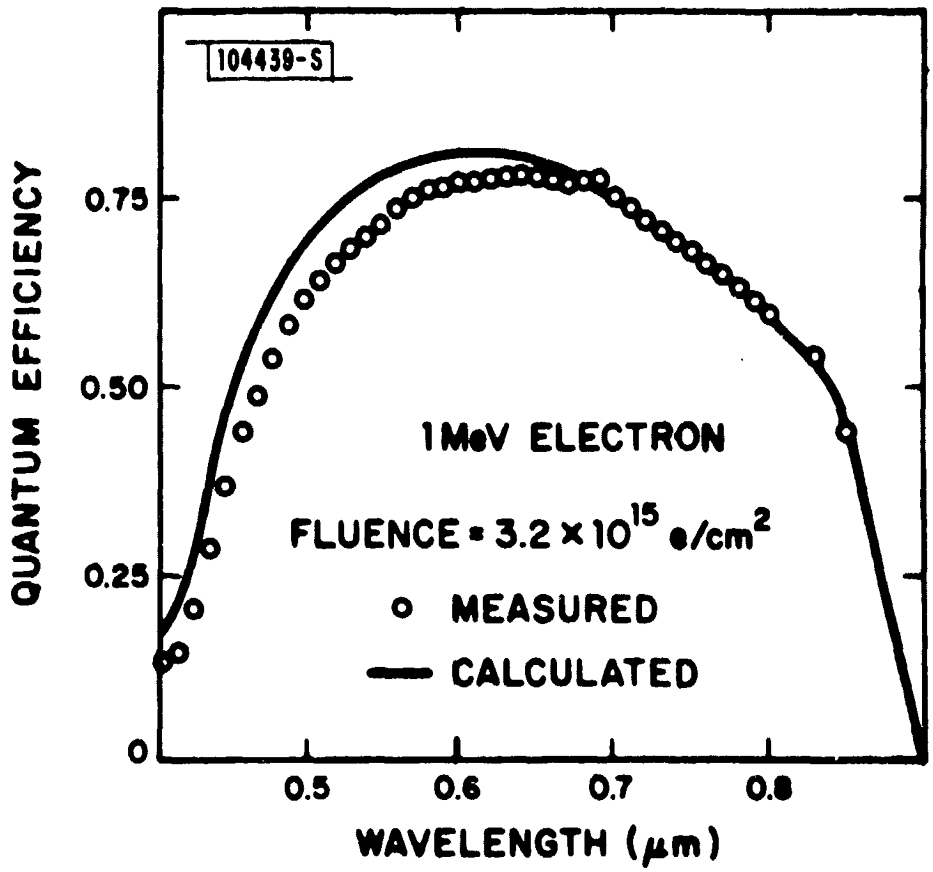

Fig. 9. Calculated and measured quantum efficiency results for cell 1 at 3.2×10^{15} e/cm^2 electron fluence.

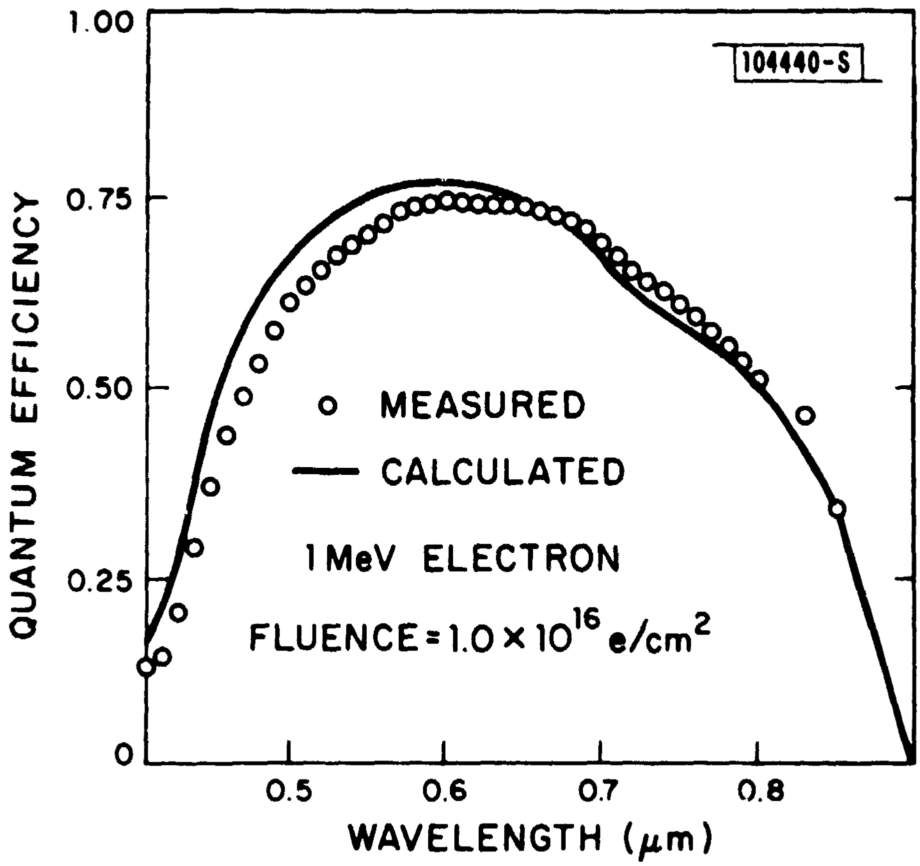

Fig. 10. Calculated and measured quantum efficiency results for cell 1 at 10^{16} e/cm^2 electron fluence.

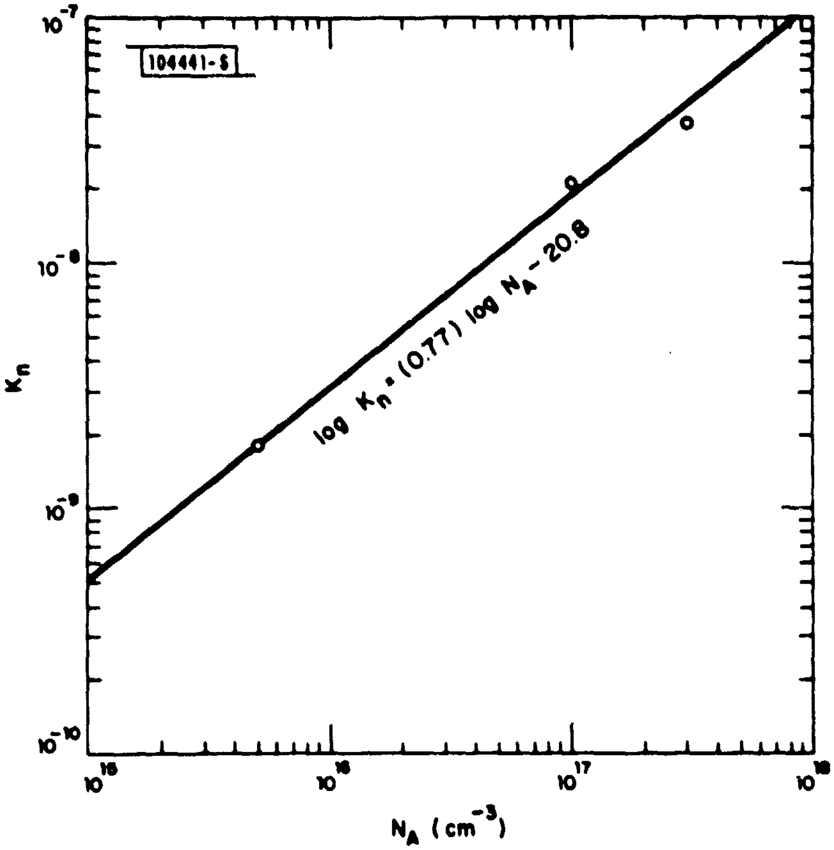

Fig. 11. Plot of damage coefficient $K_n\phi$ as a function of doping levels in p-type GaAs.

TABLE VI

CALCULATED SOLAR CELL CHARACTERISTICS UNDER 1-MeV ELECTRON IRRADIATION

Doping in p Layer N_A (cm^{-3})	Initial Values				Final Values (After 10^{16} e/cm^2)			
	J_{sc} (mA/cm^2)	V_{oc} (V)	ff	η (percent) (AM0)	J_{sc} (mA/cm^2)	V_{oc} (V)	ff	η (percent) (AM0)
1.0×10^{15}	28.8	0.975	0.820	17.0	28.6	0.805	0.787	13.40
5.0×10^{15}	28.7	0.985	0.822	17.2	27.4	0.815	0.790	13.10
1.0×10^{16}	28.7	0.990	0.822	17.3	26.5	0.820	0.790	12.70
5.0×10^{16}	28.6	0.995	0.827	17.5	23.6	0.830	0.792	11.50
1.1×10^{17}	28.6	1.000	0.824	17.5	22.1	0.835	0.790	10.80
5.0×10^{17}	28.2	1.000	0.826	17.3	18.2	0.840	0.794	8.98

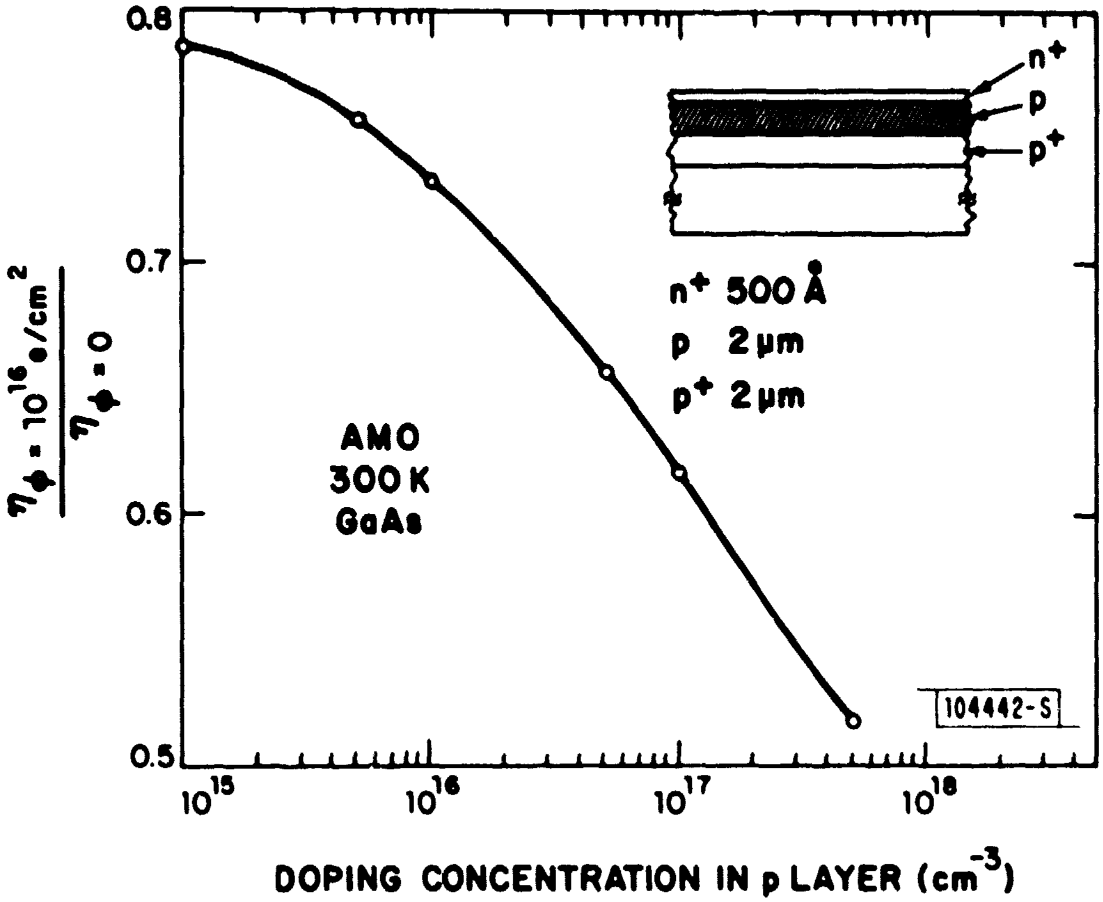

Fig. 12. Plot of ratios of calculated AM0 efficiencies for GaAs $n^+/p/p^+$ solar cells before and after 10^{16} e/cm^2 1-MeV electron irradiation as a function of doping levels N_A in p layers of cells.

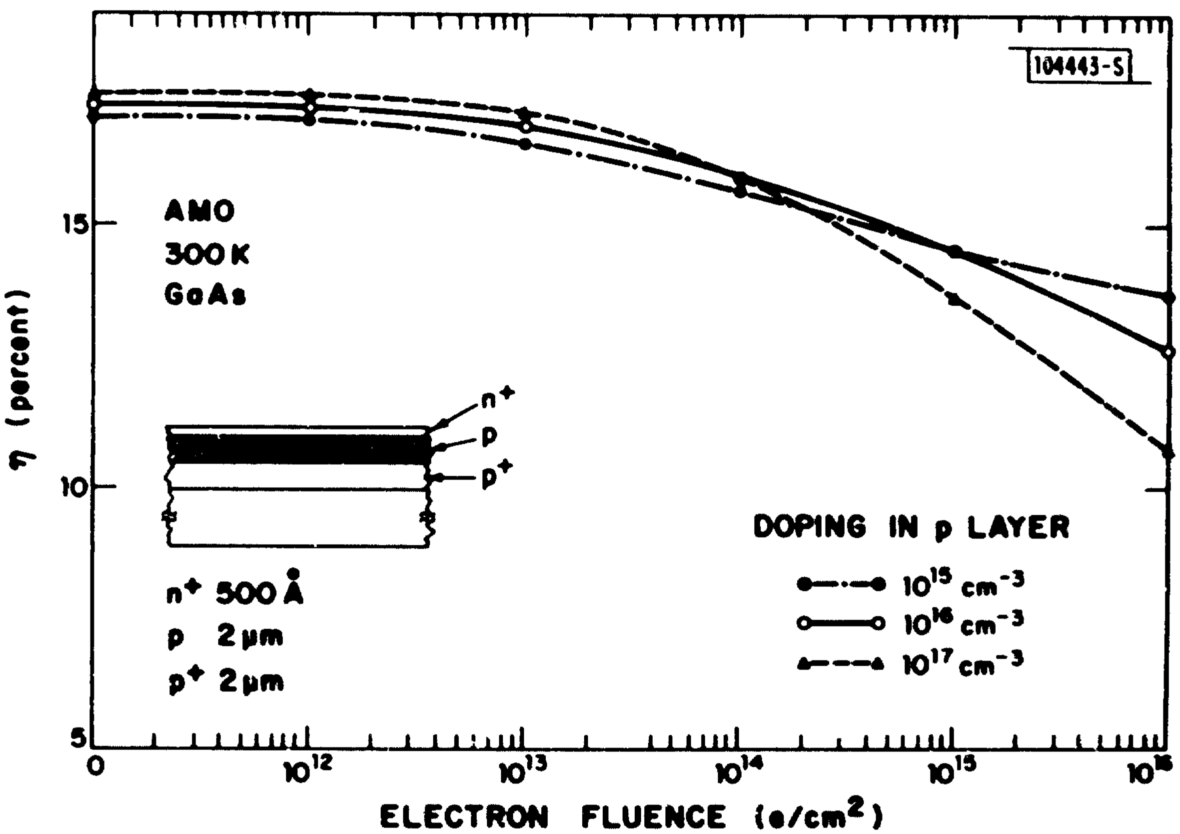

Fig. 13. Calculated conversion efficiencies at AM0 for $n^+/p/p^+$ GaAs shallow-homojunction solar cells as a function of electron fluence. Three different doping levels N_A in p layers were used.

VI. SUMMARY

In summary, we have succeeded in fabricating 2- × 2-cm GaAs $n^+/p/p^+$ shallow-homojunction solar cells with conversion efficiencies close to 16 percent at AM0. With more optimal cell designs and a better antireflection coating, we are confident that efficiencies over 1[illegible] percent at AM0 can be obtained.

In addition, our analysis of 1-MeV electron irradiation results indicates that the doping levels in the p layer of our cells are the most important parameter in determining the resistance of such cells to 1-MeV electron irradiation. A doping level of between 10^{15} and 10^{16} cm^{-3} in the p layer will provide cells with almost as high conversion efficiencies as those cells doped to 10^{17} cm^{-3}, but will have much better resistance to 1-MeV electron irradiation.

REFERENCES

1. J. M. Woodall and H. J. Hovel, J. Vac. Sci. Technol. 12, 1000 (1975).
2. J. J. Wysocki and P. Rappaport, J. Appl. Phys. 31, 571 (1960).
3. N. J. Nelson, K. K. Johnson, R. L. Moon, H. Y. Vanderplas, and L. W. James, Appl. Phys. Lett. 33, 26 (1978).
4. J. C. C. Fan, R. L. Chapman, C. O. Bozler, and P. J. Drevinsky, Appl. Phys. Lett. 36, 53 (1980).
5. C. Stuerke, Conference Record of 13th IEEE Photovoltaic Specialists Conference, Washington, DC, June 1978 (IEEE, New York, 1978), p. 551.
6. G. H. Walker, C. E. Byvik, E. J. Conway, J. H. Heinbockel, and M. J. Doviak, J. Electrochem. Soc. 125, 2034 (1978).
7. G. S. Kamath, J. Ewan, and R. C. Knechti, IEEE Trans. Electron Devices ED-24, 473 (1977).
8. J. M. Woodall and H. J. Hovel, Appl. Phys. Lett. 30, 492 (1977).
9. J. C. C. Fan, C. O. Bozler, and R. L. Chapman, Appl. Phys. Lett. 32, 390 (1978), DDC AD-A058281/7.
10. C. O. Bozler, J. C. C. Fan, and R. W. McClelland, Chapter 5 in Gallium Arsenide and Related Compounds (St. Louis) 1978 (The Institute of Physics, London, 1979), pp. 429-436, DDC AD-A072370/0.
11. M. P. Thekakeara, Solar Energy 14, 109 (1973).
12. A. Meulenberg, D. J. Curtin, and R. W. Cool, Conference Record of the 12th IEEE Photovoltaic Specialists Conference, Baton Rouge, LA, 1976 (IEEE, New York, 1976), p. 238.
13. S. Kamath and G. Wolff, U. S. Air Force Report No. AFAPL-TR-78-96, 1979.
14. G. H. Walker and E. J. Conway, J. Electrochem. Soc. 125, 1726 (1978).
15. J. C. C. Fan, C. O. Bozler, and B. J. Palm, Appl. Phys. Lett. 35, 875 (1979), DDC AD-A085501/5.
16. R. J. Chaffin, Microwave Semiconductor Devices: Fundamentals and Radiation Effects (Wiley, New York, 1973).